

Inhibition of Cellular Autophagy Deranges Dengue Virion Maturation

Roberto Mateo,^a Claude M. Nagamine,^b Jeannie Spagnolo,^a Ernesto Méndez,^{c†} Michael Rahe,^a Michael Gale, Jr.,^d Junying Yuan,^e Karla Kirkegaard^a

Department of Microbiology and Immunology,^a Department of Comparative Medicine,^b Stanford University School of Medicine, Stanford, California, USA; Departamento de Genética del Desarrollo y Fisiología Molecular, Instituto de Biotecnología, Universidad Nacional Autónoma de México, Cuernavaca, Morelos, Mexico^c; Department of Immunology, University of Washington, Seattle, Washington, USA^d; Department of Cell Biology, Harvard Medical School, Boston, Massachusetts, USA^e

Autophagy is an important component of the innate immune response, directly destroying many intracellular pathogens. However, some pathogens, including several RNA viruses, subvert the autophagy pathway, or components of the pathway, to facilitate their replication. In the present study, the effect of inhibiting autophagy on the growth of dengue virus was tested using a novel inhibitor, spautin-1 (specific and potent autophagy inhibitor 1). Inhibition of autophagy by spautin-1 generated heat-sensitive, noninfectious dengue virus particles, revealing a large effect of components of the autophagy pathway on viral maturation. A smaller effect on viral RNA accumulation was also observed. Conversely, stimulation of autophagy resulted in increased viral titers and pathogenicity in the mouse. We conclude that the presence of functional autophagy components facilitates viral RNA replication and, more importantly, is required for infectious dengue virus production. Pharmacological inhibition of host processes is an attractive antiviral strategy to avoid selection of treatment-resistant variants, and inhibitors of autophagy may prove to be valuable therapeutics against dengue virus infection and pathogenesis.

All positive-strand RNA viruses, including picornaviruses, such as poliovirus, rhinovirus, and hepatitis A virus, and flaviviruses, such as dengue virus and hepatitis C virus (HCV), rely heavily on cellular membranes at numerous stages of their infectious cycles. For example, RNA replication complexes must assemble on the topologically cytoplasmic surfaces of intracellular membranes. In some cases, such as poliovirus and hepatitis A virus, these RNA replication complexes are on the convex outer surfaces of discrete vesicles (1). In others, such as dengue virus, RNA replication complexes are assembled on invaginated membrane surfaces that are connected to the cytosol only via narrow openings (2, 3). For dengue virus, newly synthesized viral RNA exits the invaginated cytoplasm and interacts with core protein, which encapsidates the viral RNA and decorates the surfaces of nearby lipid droplets via the high-affinity binding of its N-terminal domain (4, 5). For HCV, a similar interaction of the core protein with lipid droplets has been described and seems to play a critical role in the assembly of viral particles (6–9). During dengue virus infection, formation of the nucleocapsid, subsequent interaction with envelope proteins, and budding into the ER lumen are likely to occur in close proximity (2). In the *cis*-Golgi, the virion undergoes a conformational change, and the viral prM (pre-matrix) protein is cleaved by the cellular furin protease into the mature M (matrix) protein and a peptide (pr) (10, 11). Upon cleavage, the pr peptide dissociates from the virion, resulting in the formation of mature progeny viruses that are highly infectious. This finely tuned interplay between cellular membrane remodeling, cellular lipid storage, and viral assembly is not only a fascinating cell biological puzzle, but also provides exciting opportunities for the development of antiviral compounds.

The cellular autophagy pathway, originally discovered as a response to starvation, provides a route for cytoplasmic constituents to be targeted to the lysosomal machinery for degradation (reviewed in reference 12). Nascent autophagosomes comprise cellular cytoplasm surrounded by two lipid bilayers that fuse from a C-shaped structure (12–14). These nascent autophagosomes con-

tain a modified form of the autophagy protein LC3. Originally characterized as microtubule-associated protein light chain 3 (MAP-LC-3), the LC3 protein is cleaved after synthesis by the cellular protease Atg4, generating an 18-kDa species termed LC3-I. When autophagy is activated, a series of covalent transfers links LC3 to the Atg7 protein, then to the Atg3 protein, and finally to phosphatidylethanolamine, generating a lipidated species termed LC3-II (15–17). This modification allows LC3 to become membrane associated, preferentially marking the developing and newly formed autophagosomes (18). The ability of the autophagy pathway to target cytoplasmic constituents to the lysosomal pathway allows turnover of damaged mitochondria and other organelles; clearance of aggregated proteins; maintenance of a favorable cellular energetic balance by degrading proteins, lipids, and glycogen; and the destruction of certain intracellular pathogens (19, 20). Autophagy has thus been hailed as a branch of the innate immune response. However, some viruses have been shown to benefit from the cellular autophagy pathway. Our laboratory (1, 21–23) and others (24) have shown that the membranous vesicles induced during poliovirus infection display several hallmarks of cellular autophagosomes: double-membrane morphology, cytoplasmic contents, and the presence of LC3-II and LAMP-1. Recent reports have shown evidence that members of the family *Flaviviridae*, such as HCV and dengue virus, also utilize components of the cellular autophagy pathway for their own growth benefit (25–29).

Assessing the importance of autophagy in the growth of any

Received 14 August 2012 Accepted 14 November 2012

Published ahead of print 21 November 2012

Address correspondence to Karla Kirkegaard, karlak@stanford.edu.

† Deceased.

This paper is dedicated to Ernesto Méndez.

Copyright © 2013, American Society for Microbiology. All Rights Reserved.

doi:10.1128/JVI.02177-12

these pathogens has been hampered by the lack of selective small-molecule inhibitors of the pathway. Until recently, the only available small-molecule inhibitor of the pathway was 3-methyladenine (3-MA), which has a working concentration in the millimolar range and inhibits multiple forms of phosphatidylinositol 3-kinases (PI3Ks). However, a high-throughput, image-based approach has recently been employed to screen a chemical library of compounds known to be bioactive for the ability of any of them to regulate the autophagy pathway. Several inducers were discovered in the screen, including nicardipine, used in the present study (30). In addition, one inhibitor, MBCQ [4-((3,4-methylenedioxybenzyl)amino)-6-chloroquinazoline], was identified and subsequently derivatized into an effective and selective autophagy inhibitor termed spautin-1 (specific and potent autophagy inhibitor 1) (31). Spautin-1 was shown to inhibit the deubiquitination activities of USP10 and USP13, which normally function to reverse the ubiquitination and subsequent degradation of the beclin-Vps34-Atg14 complex, which is essential in the early stages of autophagy. The degradation of beclin-Vps34-Atg14 complexes promoted by spautin-1 treatment also decreases the intracellular concentrations of phosphatidylinositol 3-phosphate (PI3P), an essential lipid component of the membranes required for the initiation of autophagosome formation (31).

The high selectivity of spautin-1 in inhibiting the autophagy pathway (31) prompted us to reevaluate the role of this cellular process in dengue virus growth. We also investigated the effect of inducing the pathway in tissue culture and in AG129 mice, a well-established model of infection that reproduces several of the major pathologies of human infection (32–34). Stimulation of autophagy generated larger amounts of infectious virus both in cells and in animals that correlated with increased pathogenicity in the mice. Inhibition of autophagy, on the other hand, generated drastically reduced amounts of infectious virions, instead producing an abundance of noninfectious particles with apparent maturation defects. Our results show that components of the autophagy pathway are not only involved in viral RNA synthesis, but, more importantly, play a critical role in the generation of infectious viral particles.

MATERIALS AND METHODS

Cells and viruses. Baby hamster kidney cells (BHK-21, clone 15) and human HeLa cells were cultured as monolayers in Dulbecco's modified Eagle's medium supplemented with 10% (vol/vol) calf serum, 100 units of penicillin/ml, 100 µg of streptomycin/ml, and 10 mM HEPES at 37°C and 5% CO₂. Human Huh7.A.1 cells were cultured in a similar fashion with 10 mM sodium pyruvate, nonessential amino acids, and 10% (vol/vol) fetal bovine serum (FBS). Huh7.A.1-green fluorescent protein (GFP)-LC3 cells were generated after three rounds of cloning and amplification of individual Huh7.A.1 colonies that stably expressed GFP-LC3. Huh7.A.1-GFP-LC3 culture medium was identical to that of Huh7.A.1 cells but also contained 1 mg/ml of Geneticin as a selectable marker. *Aedes albopictus* C6/36 cells were cultured as monolayers in Leibovitz's L-15 medium supplemented with 10 mM HEPES, 100 units of penicillin/ml, 100 µg streptomycin/ml, and 10% (vol/vol) fetal bovine serum at 30°C.

Dengue virus type 2 (DENV2) 16681 was propagated from an infectious cDNA clone (pD2/IC, a gift from Eva Harris, University of California [UC], Berkeley). DENV2 PL046 was also generated from infectious cDNA (a gift from Sujana Shrestha, La Jolla Institute for Allergy and Immunology). All viruses were grown in C6/36 cells, and their titers were determined in BHK-21 cells. For mouse experiments, virus was concentrated at 53,000 × g for 2 h at 4°C and resuspended in cold, endotoxin-free phosphate-buffered saline (PBS) supplemented with 10% fetal bovine serum.

Hepatitis C virus JFH1 serotype 2a was generated after electroporation of susceptible Huh7.5 cells with an infectious cDNA clone synthesized to correspond to the sequence of JFH1 (35). Concentrated virus stocks were prepared by filtration of supernatants from infected Huh7.5 cells through a Centricon Plus-70 filter (Millipore, Billerica, MA).

Poliovirus type 1 Mahoney was propagated from an infectious cDNA plasmid as previously described (36).

Antibodies. Anti-dengue virus antibodies against all four serotypes of dengue virus or against prM were purchased from Abcam (Cambridge, MA). Anti-LC3 antibody was purchased from Sigma (St. Louis, MO). Anti-glyceraldehyde-3-phosphate dehydrogenase (GAPDH) antibody was purchased from Santa Cruz Biotechnology (Santa Cruz, CA).

Plasmids and RNA transcription. The region of the pD2/IC plasmid containing the DENV2 16681 genome was cut into three fragments and subcloned into a pUC18 backbone for easier manipulation (SacI and SphI sites for subclone 1, SphI and KpnI sites for subclone 2, and KpnI and XbaI sites for subclone 3). Mutagenesis of the viral genome was performed in the appropriate subclone plasmid by site-directed mutagenesis using the QuikChange site-directed mutagenesis kit (Agilent Technologies, Santa Clara, CA). Each amplified DNA segment was sequenced in its entirety to ensure that no adventitious mutations were introduced and was subcloned back into the infectious cDNA backbone to generate infectious RNA. Infectious RNAs were generated by *in vitro* transcription with the MEGascript T7 kit (Ambion) with the following modifications to the manufacturer's protocol: 5 mM each GTP, CTP, and UTP; 1 mM ATP; and 5 mM 7mG(5')ppp(5')A cap analog incubated for 4 h at 30°C with the addition of 2 mM ATP after 30 min. Free nucleotides were removed by gel filtration chromatography on a Micro Bio-Spin P-30 Tris column (Bio-Rad Laboratories, Hercules, CA). All DNA templates were generated by digestion with XbaI, phenol-chloroform extracted, and ethanol precipitated using standard procedures.

Protein extraction and immunoblotting. Protein extraction from cultured cells or mouse tissues has been described elsewhere (37). Briefly, tissues harvested from mice were resuspended in PBS in the presence of complete EDTA-free protein inhibitors (Roche Applied Bioscience, Indianapolis, IN). Cell lysates were separated by sodium-dodecyl sulfate (SDS)-polyacrylamide gel electrophoresis on a 15% acrylamide gel and transferred to Immobilon polyvinylidene difluoride (PVDF) membranes (Millipore, Billerica, MA) for 60 min at 100 V in a Miniprotean III transfer tank (Bio-Rad, Hercules, CA). Viral particles from total supernatants were collected by centrifugation at 53,000 × g for 2 h at 4°C and resuspended in TNE buffer (12 mM Tris, pH 8, 120 mM NaCl, and 1 mM EDTA). Immunoblots were incubated with anti-LC3 antibody (Sigma) or anti-prM antibody (Abcam) at a dilution of 1/1,000 (or 1/5,000 for anti-GAPDH antibody), followed by incubation with alkaline phosphatase-conjugated goat anti-rabbit (LC3), rabbit anti-goat (GAPDH), or goat anti-mouse (prM) immunoglobulin (Jackson ImmunoResearch, West Grove, PA) at a dilution of 1/10,000. The immunoblots were imaged on a phosphorimager (Bio-Rad), and band quantitation was conducted with ImageQuant software (Bio-Rad).

RNA transfections. BHK-21 cells were seeded in 24-well plates, grown to 80% confluence, and transfected with 1 to 2 µg of RNA using Lipofectamine 2000 (Invitrogen, Grand Island, NY), followed by a 4-h incubation at 37°C in 5% CO₂. At that point, the RNA was removed, and the cells were washed three times in 1 ml culture medium and then incubated for a total of 48 to 72 h. The supernatants were collected after a quick clarification of cell debris, and the viral titer was assessed by plaque assay.

qRT-PCR. Extracellular RNA was extracted with the RNeasy Mini Kit (Qiagen, Valencia, CA). Intracellular RNA from infected cells was isolated in a similar way after three freeze-thaw cycles. Viral RNA from sucrose fractions was precipitated after phenol-chloroform extraction. Briefly, 200 µl of sample was treated with 200 µg/ml proteinase K and 0.1% (wt/vol) SDS for 1 h at 37°C. Samples were then phenol-chloroform extracted twice, ethanol precipitated, and resuspended in nuclease-free water. Quantitative reverse transcription (qRT)-PCR of viral RNA was per-

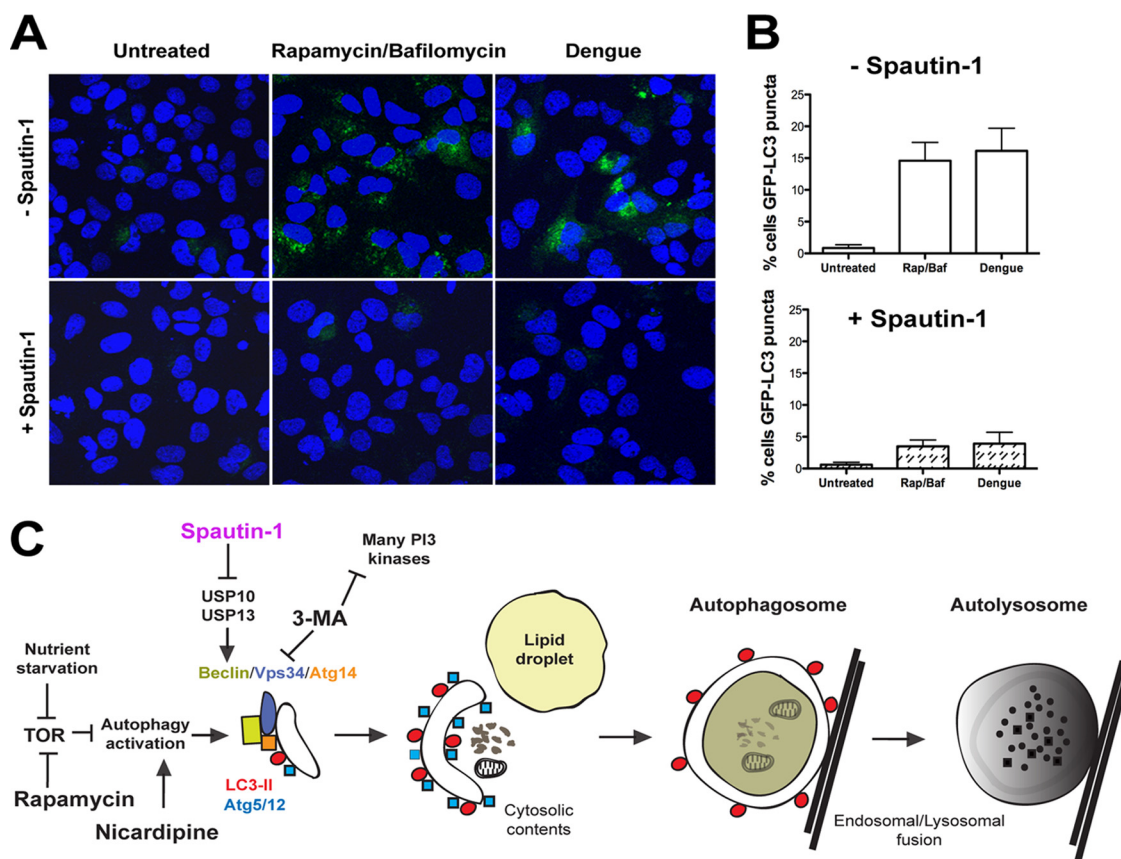


FIG 1 Effect of spautin-1 on the formation of rapamycin-induced autophagosomes and dengue virus-induced LC3-containing membranous structures. (A) Huh7.A.1-GFP-LC3 cells were untreated, treated with 0.5 μ M rapamycin and 50 nM bafilomycin, or infected with dengue virus at an MOI of 0.1 in either the presence (+) or absence (–) of 10 μ M spautin-1. Images were taken after a 24-hour incubation period. Nuclei were visualized by DAPI staining. (B) The percentage of GFP-LC3-containing cells was calculated in 10 random fields. Shown are the averages \pm standard errors of the mean (SEM). (C) Overview of the autophagy pathway with the drugs used in this study and their targets.

formed on an Applied Biosystems 7300 machine using the QuantiTect SYBR Green RT-PCR Kit (Qiagen) with anti-DENV2 NS4B primers. Primer sequences are available upon request.

Infectivity assays. Virus titrations were conducted on BHK-21 cells. Briefly, BHK-21 monolayers were grown to 70% confluence in 24-well plates and incubated with serially diluted virus supernatants for 1 h at 37°C in 5% CO₂. The wells were subsequently overlaid with Dulbecco's modified Eagle's medium, 1% SeaPlaque low-melting-point agarose (Cambrex, Rockland, ME), and 5% FBS; incubated for 3 days; and fixed with 10% formaldehyde. The cells were then permeabilized with methanol for 10 min, washed with PBS, and immunostained using a rabbit anti-DENV1, -2, -3, -4 antibody (Abcam) and a horseradish peroxidase (HRP)-goat anti-rabbit secondary antibody. After incubation of the substrate (3-amino-9-ethyl carbazole) for 10 to 20 min at 37°C, foci were counted under the microscope, and focus-forming units (FFU) per ml were calculated.

Velocity centrifugation. Gradients were generated using a gradient station (model 153; Biocomp, Fredericton, NB, Canada) following the manufacturer's instructions. Viral supernatants were loaded onto 5 to 50% (wt/wt) sucrose gradients and centrifuged for 16 h at 100,000 \times g at 4°C, after which they were fractionated into 1-ml aliquots. The amount of virus in each aliquot was directly quantitated in BHK-21 cells; viral RNA was extracted as described above.

Mouse infections. AG129 mice (129/Sv mice lacking alpha/beta interferon [IFN- α / β] and IFN- γ receptors), obtained from Harry Greenberg (Stanford University School of Medicine), were bred and housed under

specific-pathogen-free conditions at the Stanford University animal care facility, which is accredited by the Association for the Assessment and Accreditation of Laboratory Animal Care, Int. The AG129 mouse colony was monitored for adventitious viral, bacterial, and parasitic pathogens by a sentinel dirty-bedding program. Sentinels are euthanized and screened for pathogens every 4 months. The sentinel mice were found to be free of mouse hepatitis virus, mouse rotavirus (EDIM), mouse parvovirus, minute virus of mice, ectromelia virus, Sendai virus, mouse parvovirus, pneumonia virus of mice, respiratory enteric virus III (Reo3), Theiler's murine encephalomyelitis virus, lymphocytic choriomeningitis virus, mouse adenovirus types 1 and 2, *Mycoplasma pulmonis*, fur mites, and pinworms. All experiments were approved by Stanford's Institutional Animal Care and Use Committee (Administrative Panel of Laboratory Animal Care). Age- and sex-matched mice at 8 to 11 weeks of age were used for all experiments. Virus (10⁷ FFU) in 10% FBS in PBS was injected retro-orbitally in a volume of 100 μ l unless otherwise indicated; mice not receiving virus received an equal volume of 10% FBS in PBS injected similarly. Drug treatments were performed intraperitoneally. For survival studies, mice were euthanized when moribund or upon initial signs of paresis/paralysis.

Confocal microscopy. Quantitation was performed by averaging 10 random fields, containing approximately 100 cells, for each condition. Images were taken on a Zeiss LSM510 Meta inverted confocal microscope.

Autophagy stimulation and inhibition. Stocks of rapamycin (Cell Signaling Technology, Danvers, MA, and LC laboratories, Woburn, MA) and nicardipine (Sigma-Aldrich) were prepared in dimethyl sulfoxide

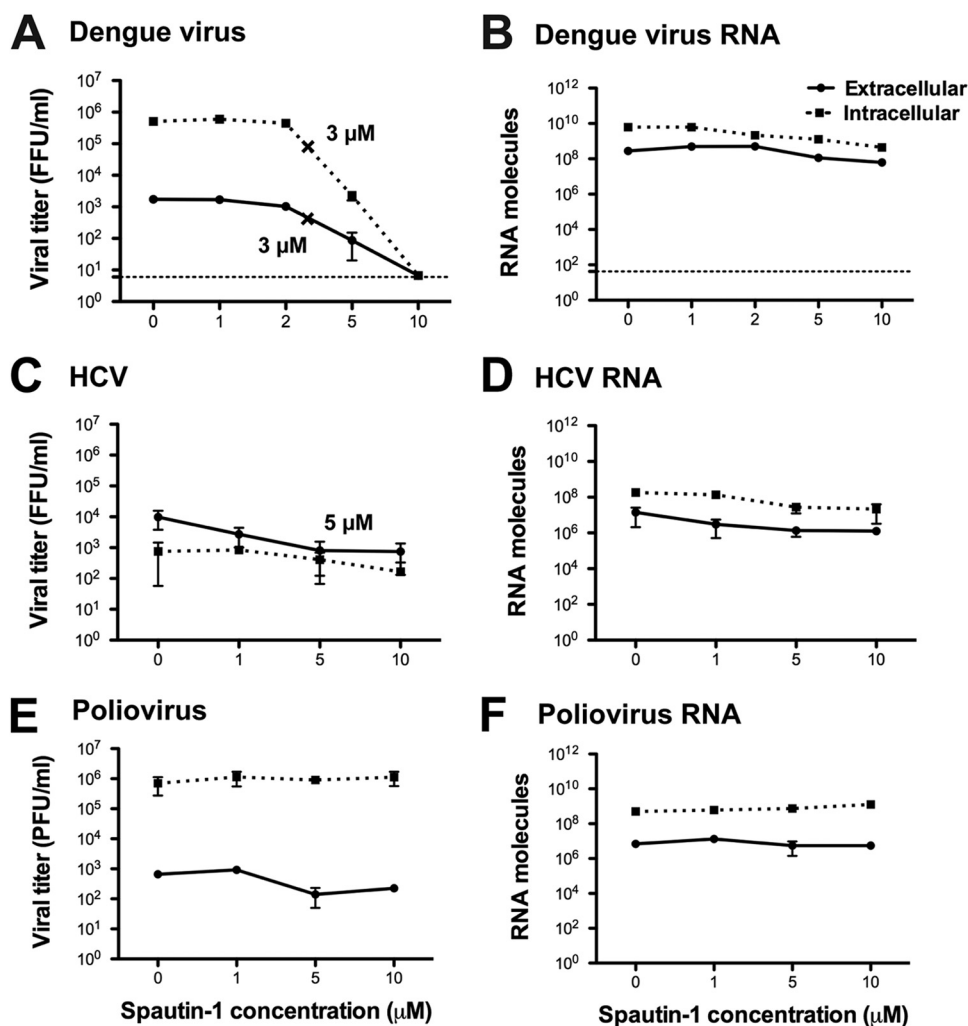


FIG 2 Effects of spautin-1 on dengue virus, HCV, and poliovirus titers and RNA. (A and B) BHK-21 cells were infected with dengue virus at an MOI of 0.1 FFU/cell and left untreated or treated with various spautin-1 concentrations for 24 h. Extracellular and intracellular titers were determined (A), and amounts of viral RNA were quantitated using qRT-PCR (B). (C and D) Huh7.5.1 cells were infected with HCV at an MOI of 0.1 FFU/cell and left untreated or treated with various spautin-1 concentrations for 72 h. Extracellular and intracellular virus titers (C) and viral RNA (D) were quantified. (E and F) HeLa cells were infected with poliovirus at an MOI of 0.1 PFU/cell and left untreated or treated with spautin-1 for 6 h. Virus titers (E) and viral RNA (F) amounts were determined. When spautin-1 was less than 10 μM, IC₅₀ values are indicated for all three viruses. All data shown are averages ± SEM of three or four biological replicates.

(DMSO) and used as autophagy stimulators in tissue culture and in mice. Spautin-1, used as an autophagy inhibitor, was also dissolved in DMSO. For tissue culture treatments, 7×10^6 BHK cells on 60-mm dishes were pretreated with either drug (or DMSO as a negative control) for 30 min at 37°C and infected at a multiplicity of infection (MOI) of 0.1 FFU per cell. Infections were always performed in duplicate. Supernatants were harvested after 24 h, and titers were determined on fresh BHK-21 cells as described above. For mouse experiments, the drugs were delivered intraperitoneally in a solution containing the drug in DMSO (5%) combined with Solutol HS15 (Sigma-Aldrich) (25%) and saline (70%). For rapamycin and nicardipine, mice were treated every 12 h for 48 h, after which spleens, leg muscles, and stomachs were collected.

Statistical analysis. Data were analyzed with Prism software (GraphPad Software, Inc.). For survival studies, Kaplan-Meier survival curves were analyzed by the log-rank test. Statistical significance was determined by using the two-tailed paired *t* test for *in vitro* experiments and the Mann-Whitney test for mouse experiments, as well as for viral RNA per FFU comparisons.

RESULTS

Spautin-1 reduces the formation of both bona fide autophagosomes and dengue virus-induced LC3-containing puncta. To test whether spautin-1, known to be an effective autophagy inhibitor, also prevents the induction of LC3-containing puncta during dengue virus infection, we tested its effects in a human hepatoma-derived cell line, Huh7.A.1 (38), that constitutively expresses GFP-LC3. The presence of GFP-LC3 puncta in cells treated with rapamycin and bafilomycin was monitored in the presence and absence of 10 μM spautin-1 (Fig. 1A). Rapamycin is known to induce autophagy, and bafilomycin arrests autophagosome maturation, thus prolonging the half-life of the punctate GFP-LC3 signal.

Untreated Huh7.A.1-GFP-LC3 cells showed low fluorescence in their cytoplasm; only about 2% of the cells displayed GFP-LC3 puncta. However, when these cells were treated with rapamycin

and bafilomycin, the percentage with GFP-LC3 puncta increased to about 15% (Fig. 1B). Pretreatment with spautin-1 before the addition of the drugs reduced the percentage of GFP-LC3-containing cells to 4%, consistent with inhibition of bona fide autophagosome formation by spautin-1 (Fig. 1B) (31).

To determine whether spautin-1 would have the same inhibitory effect on dengue virus-induced GFP-LC3-containing structures, we monitored changes in infected cells with and without spautin-1 treatment. When cells were infected at an MOI of 0.1 FFU per cell, the expected 10% of cells displayed cytoplasmic GFP-LC3 puncta, consistent with the cell-autonomous induction of autophagosome-like structures previously observed during dengue virus infection (26–28). On the other hand, when cells were treated with spautin-1 before and during infection with dengue virus, a large reduction in the prevalence and intensity of the GFP-LC3 puncta was observed (Fig. 1A and B). This indicates that spautin-1 alters the formation of both bona fide autophagosomes and dengue virus-induced GFP-LC3-containing membranous structures.

Inspection of the autophagy pathway (Fig. 1C) reveals that the known destabilization of the beclin-Vps34-Atg14 complex by spautin-1 (31) should inhibit formation of Atg5-Atg12 complexes, LC3-II formation, autophagosome formation, and all downstream steps. Presumably, dengue virus hijacks some aspect of the pathway, like the beclin-Vps34-Atg14 complex or some downstream component, for its infectious cycle. Previous work has suggested that viral RNA replication was one step of the dengue virus life cycle dependent on the autophagy pathway (26).

Spautin-1 specifically reduces infectious dengue virus titers in BHK-21 cells. To investigate the effect of spautin-1 on viral replication in tissue culture, we tested its effects on dengue virus growth in BHK-21 cells, in which the virus grows to higher titers in single-cycle infections than in Huh7 cells and which therefore provide more dynamic range to test the effects of inhibitors. BHK-21 cells were infected at an MOI of 0.1 FFU per cell, after which incubation was continued in the presence of spautin-1. Supernatants and cells were harvested after 24 h, and titers were determined for the presence of virus in both the extracellular and intracellular compartments. Treatment with a range of concentrations of spautin-1 showed profound, dose-dependent inhibition of the yield of infectious virus, both extracellular and intracellular, with statistically significant drops in titers of several orders of magnitude at the highest spautin-1 concentrations. The 90% inhibitory concentration (IC₉₀) values of 3 μM for both these effects indicate that spautin-1, although a useful reagent for investigating the influence of autophagy on cellular and infectious processes, will need further development to be a useful pharmacological reagent in humans or, in fact, in mice.

To determine whether the large decreases in viral titer caused by spautin-1 were due to early events, such as translation and RNA replication, that would affect the amount of viral RNA, RNA was extracted and quantified using qRT-PCR. Interestingly, at 10 μM spautin-1, the amount of viral RNA was only about 10-fold lower than in the absence of the compound in both the extracellular and intracellular compartments (Fig. 2B). Therefore, the reduced yield of infectious virus upon spautin-1 treatment could not be exclusively attributed to a defect in translation or viral RNA synthesis. We hypothesized that the accumulated RNA was present in non-infectious structures either within or outside the cells.

As HCV and poliovirus have also been reported to subvert the

TABLE 1 Specific infectivities of dengue virus, hepatitis C virus, and poliovirus in the absence and presence of spautin-1

Virus	Spautin-1 concn (μM)	Specific infectivity ^a	
		Extracellular	Intracellular
Dengue virus	0	44 ± 8	572 ± 120
	1	24 ± 2	676 ± 94
	2	14 ± 3	1,450 ± 445
	5	5 ± 4	13 ± 5
	10	0.8 ± 0.1	0.1 ± 0.07
Hepatitis C virus	0	48 ± 70	0.3 ± 0.4
	1	63 ± 92	0.4 ± 0.2
	5	41 ± 59	1.2 ± 1.3
	10	40 ± 45	0.5 ± 1
Poliovirus	0	7 ± 1	100 ± 75
	1	5 ± 6	130 ± 110
	5	2 ± 2	86 ± 5
	10	3 ± 4	62 ± 40

^a For dengue virus, FFU/10⁶ RNA molecules; for HCV, FFU/10⁴ RNA molecules; for poliovirus, PFU/10⁴ RNA molecules.

autophagy pathway, we tested whether spautin-1-mediated instability of the beclin-Vps34-Atg14 complex would be inhibitory to these viruses. The yield of infectious HCV was reduced only 10-fold at the highest spautin-1 concentration (10 μM), with a similar decrease in the amount of viral RNA (Fig. 2C and D). Upon poliovirus infection, a small effect on intracellular virus and a larger effect on extracellular virus were observed (Fig. 2E and F), consistent with previous work (21, 37). Importantly, the amounts of RNA paralleled the amounts of infectious virus for both poliovirus and hepatitis C virus (Fig. 2), arguing that the effect of spautin-1 on RNA synthesis is sufficient to explain the decreased titers. For both viruses, these 5- to 10-fold effects on both virion production and RNA abundance are consistent with previous reports in which small interfering RNA (siRNA)-based methods to inhibit autophagy were employed (21, 25, 37, 39).

To quantify the effect of spautin-1 on the packaging, assembly, or maturation of viral particles, we calculated their specific infectivities, the ratio of infectious particles to the amounts of viral RNA, under increasing drug concentrations. As can be seen in Table 1, the specific infectivity of dengue virus RNA decreased greatly with increasing spautin-1 concentrations, especially in the intracellular compartment. The specific infectivities of HCV and poliovirus particles remained relatively unaffected by spautin-1 treatment. Therefore, for dengue virus, destabilizing the beclin-Vps34-Atg14 complex has a modest effect on dengue virus RNA accumulation and a much larger effect on the production of infectious virus. Conversely, treatment with rapamycin, which stimulated autophagy by inhibiting mammalian target of rapamycin (mTOR), or nicardipine, which increases autophagy by modulation of calcium flux, causes a modest but statistically significant increase in the amount of infectious dengue virus (Fig. 3A and B).

Inhibition of dengue virus infectivity by spautin-1 cannot be rescued by lipid complementation. Previous studies have shown that the approximately 10-fold inhibition of dengue yield by 3-MA can be reversed by the external addition of fatty acids to the medium (26). If this were true for all inhibitors of autophagy, it would suggest that the effect was nutritional or mediated by lipid signaling, rather than dependence on components of the au-

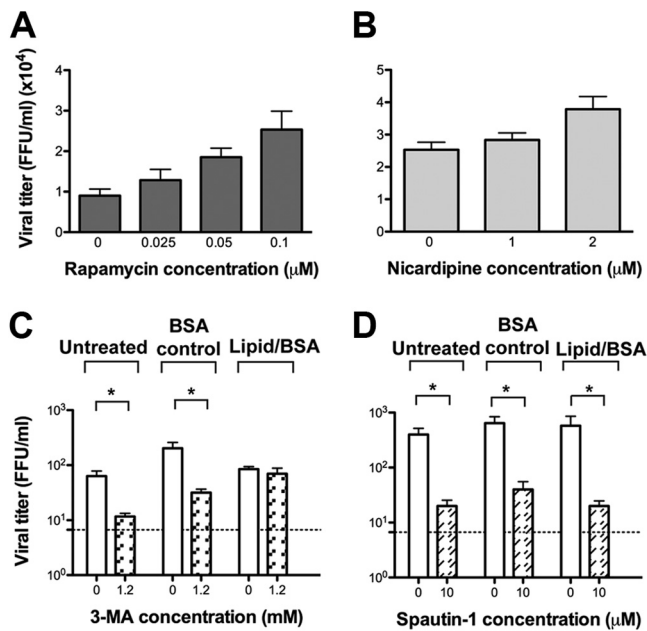


FIG 3 Effect of autophagy stimulation and fatty acid supplementation upon 3-MA and spautin-1 treatment of BHK-21 cells on extracellular dengue virus yield. (A and B) BHK-21 cells were infected with dengue virus at an MOI of 0.1 FFU/cell and treated with increasing concentrations of rapamycin (A) and nicardipine (B) for 24 h. Supernatants were collected, and titers were determined on fresh BHK-21 monolayers. Experiments representative of several performed are shown. (C and D) BHK-21 cells were similarly infected with dengue virus at an MOI of 0.1 FFU/cell and left untreated or treated with 1.2 mM 3-MA (C) or 10 μM spautin-1 (D) in the presence or absence of oleic acid-BSA or BSA alone for 24 h. Extracellular titers and SEM were determined by focus-forming-unit assay. *, $P < 0.05$. A dashed line indicates the limit of detection of 7 FFU/ml for the titration assay.

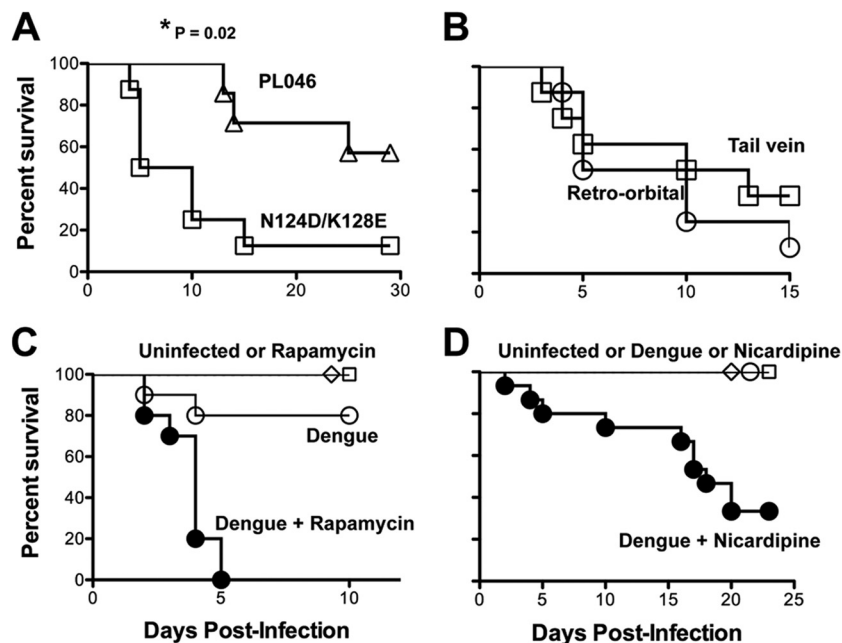


FIG 4 Pathogenicity of dengue virus in autophagy-stimulated AG129 mice. (A) AG129 mice were intravenously inoculated with 10^7 FFU/mouse of the wild-type dengue virus strain PL046 or virus containing the mutations N124D and K128E in the envelope protein (40), and a time course of lethality was determined. (B) Mice were intravenously inoculated with 10^7 FFU/mouse of dengue virus N124D/K128E via the tail vein or retro-orbitally. (C and D) Mice were retro-orbitally inoculated with 2×10^5 FFU of dengue virus N124D/K128E and treated with rapamycin (20 mg/kg) (C) or nicardipine (5 mg/kg) (D) by intraperitoneal injection every 12 h. Differences in pathogenicity between mice infected with dengue virus alone or dengue virus with rapamycin (C) or nicardipine (D) were statistically significant ($P < 0.001$ and $P = 0.01$, respectively).

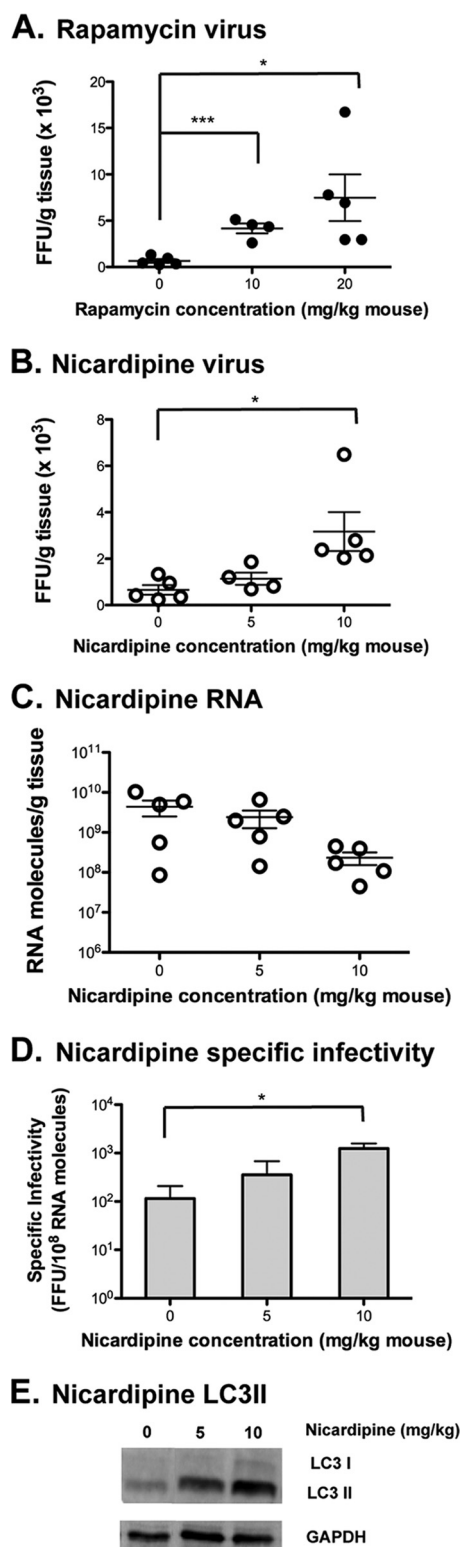


FIG 5 Effect of autophagy stimulation in AG129 mice on dengue virus and RNA accumulation. (A and B) Mice were retro-orbitally inoculated with 2×10^5 FFU/mouse of N124D/K128E dengue virus and treated with the indicated amounts of rapamycin or nicardipine every 12 h. Spleens were harvested, homogenized, and analyzed to determine the amounts of infectious virus under rapamycin (A) and nicardipine (B) stimulation. (C) Viral RNA was also determined in spleens of nicardipine-treated mice. Each point represents one individual mouse; the mean values \pm SEM are shown. (D) Spe-

and tail vein inoculations was shown (Fig. 4B). To test the effect of autophagy stimulation, mice were inoculated retro-orbitally with a sublethal dose of N124D/K128E virus (2×10^5 FFU/mouse) and treated with rapamycin (20 mg/kg of body weight) or nicardipine (5 mg/kg) by intraperitoneal (i.p.) injection every 12 h for several days. Uninfected control mice treated with the drug or vehicle solution were carried in parallel to test for potential toxicity of the treatments. As shown in Fig. 4C, treatment of infected mice with rapamycin caused greatly increased pathogenicity: all treated mice died by day 5, whereas 80% of untreated mice survived at that time. Nicardipine treatment also led to a statistically significant increase in dengue virus pathogenicity (Fig. 4D).

To test the effects of rapamycin and nicardipine on the induction of autophagy and virus production during murine infection, a time course of virus production in AG129 mice was performed. At various times postinfection, livers, spleens, and mesenteric lymph nodes were analyzed, with the spleen displaying the largest amounts of infectious virus and viral RNA. Readily quantifiable amounts of virus and viral RNA were observed in the spleen as early as 16 h postinfection, reaching a plateau at approximately 48 h postinfection (data not shown). To test the effect of autophagy stimulation, mice were retro-orbitally infected with 2×10^5 FFU per mouse and treated with rapamycin and nicardipine every 12 h for 2 days. Harvested splenic tissue showed higher titers of virus following stimulation of autophagy for both treatments (Fig. 5A and B). Specifically, at the highest rapamycin and nicardipine concentrations, viral titers were, on average, 11-fold and 5-fold higher, respectively, than in untreated mice. Given the known side effects of rapamycin on the immune response, the analysis of nicardipine-treated mice was continued. When the amounts of viral RNA in the spleen were quantified, the differences between treated and untreated samples were highly variable but not statistically significant (Fig. 5C). The apparent decrease in the amount of viral RNA concomitant with the increase in infectious virus further underscored the effect of the autophagy pathway or its components on the specific infectivity of dengue virions (Fig. 5D). To confirm the induction of autophagy by nicardipine treatment, protein homogenates were generated from muscle, a tissue with large amounts of endogenous LC3. At concentrations of 5 and 10 mg of nicardipine/kg, increased amounts of LC3-II in the muscles of treated mice were observed (Fig. 5E), consistent with the effectiveness of nicardipine in autophagy induction in the mouse.

Treatment with spautin-1 results in defective extracellular viral particles. To test directly whether components of the autophagy pathway are required for the assembly of infectious virions, the viral particles formed in tissue culture cells in the presence and absence of spautin-1 were monitored. In infected, untreated samples, coincident peaks of viral RNA and infectious virus were observed around fractions 7, 8, and 9 (Fig. 6A). When subjected to heating, the viral RNA still sedimented in those fractions (Fig. 6A), arguing that the particles remained intact following heating.

Treatment with 10 μ M spautin-1, on the other hand, resulted in the generation of multiple RNA peaks throughout the gradient

cific infectivity (FFU/ 10^8 molecules) in the spleen was determined for nicardipine-treated mice. (E) Gastrocnemius muscles were collected 48 h after infection, and protein homogenates were generated and blotted for the presence of LC3 using GAPDH as a loading control. A representative blot for nicardipine treatment is shown.***, $P < 0.0005$; *, $P < 0.05$.

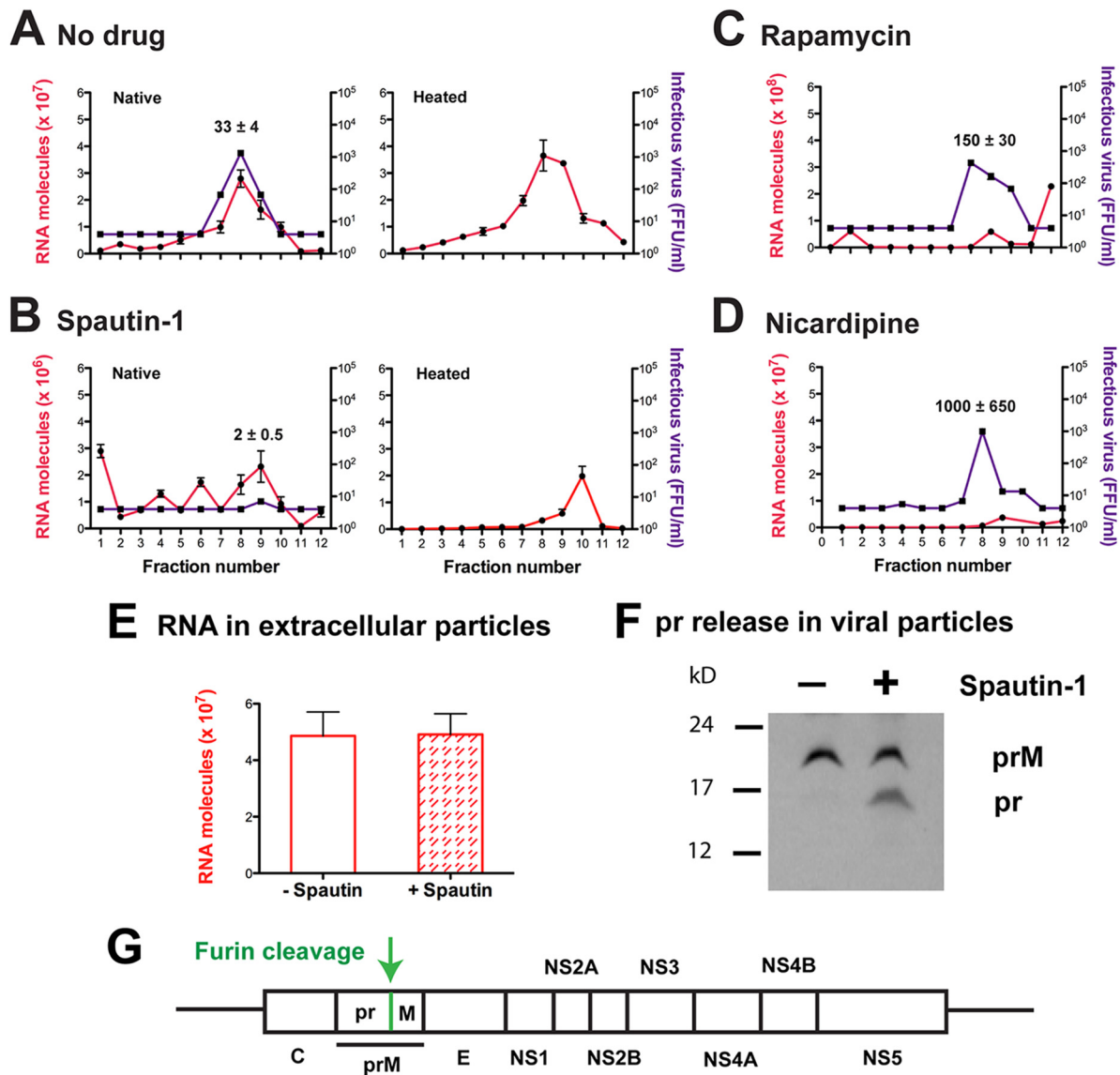


FIG 6 Analysis of dengue virus particles formed upon spautin-1, rapamycin, and nicardipine treatment. (A to D) Supernatants from dengue virus-infected BHK-21 cells that were untreated (A) or had been treated with spautin-1 (B), rapamycin (C), or nicardipine (D) were loaded onto 5 to 50% sucrose gradients and subjected to velocity centrifugation. Fractions were collected and analyzed to determine the amounts of infectious virus and viral RNA. Supernatants from spautin-1-treated cells and untreated cells were heated for 1 h at 37°C and subjected to the same velocity sedimentation. RNA was extracted from the resulting fractions, and viral RNA was quantitated. For each panel, specific activities (infectious virus/ 10^5 RNA molecules) for each condition \pm SEM are indicated over the virus and RNA peaks. (E and F) Extracellular viral particles produced upon spautin-1 treatment were pelleted. Viral RNA was extracted and quantitated by qRT-PCR (E), and particles were analyzed by Western blotting for detection of prM protein (F). (G) dengue virus genome showing the maturation cleavage in prM protein.

that were not associated with infectivity (Fig. 6B). This suggested that, under autophagy inhibition conditions, noninfectious particles of various shapes and sizes were formed that could correspond to either assembly or disassembly intermediates. To test whether these deranged particles had other altered physicochemical properties, the preparations were subjected to heat treatment. Disappearance of the slowly sedimenting species and appearance of a very sharp peak closer to the bottom of the gradient were observed. Thus, the physical properties of the deranged particles formed in the presence of spautin-1 were drastically altered compared to normal infectious virions.

To test the effect of autophagy stimulation on viral particle

formation, sedimentation profiles of the media from cells infected in the presence of rapamycin or nicardipine were analyzed (Fig. 6C and D). Infectious virus formed under these conditions sedimented similarly to infectious virions formed in the absence of drugs (Fig. 6C and D). However, the amounts of RNA in these infectious fractions were much smaller than in untreated samples. The higher specific infectivities of virions formed when autophagy was stimulated are demonstrated in Fig. 6C and D, in which the amounts of infectious virus relative to viral RNA differ greatly from those observed in the absence of these compounds (Fig. 6A).

To test directly whether viral particles produced in the presence of spautin-1 were physically altered, total supernatants of

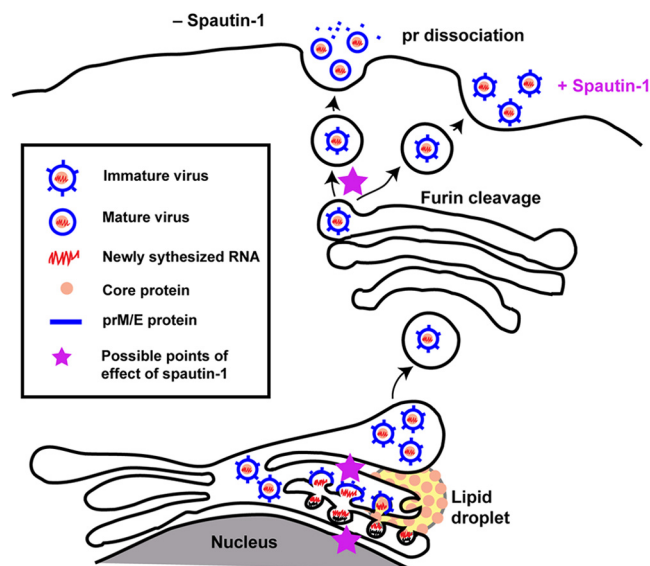


FIG 7 Model of spautin-1 action on the dengue virus life cycle. Viral RNA synthesis and formation of particles by budding into the ER are affected by spautin-1 treatment. Once immature, spiky viruses are formed in the ER lumen, they are transported via the secretory pathway through the Golgi network, where furin cleaves the structural prM protein, generating mature M protein and pr peptide, which remain associated with the virion until released in the extracellular milieu. This event produces viruses that are highly infectious. However, upon spautin-1 treatment, the pr peptide remains associated with the virions even after reaching the extracellular space, which renders them noninfectious.

cells infected in the presence and absence of spautin-1 were harvested and viral particles were collected by centrifugation. Viral RNA was quantified by qRT-PCR (Fig. 6E) and was shown to be similar in both preparations. However, viral prM-containing proteins, as visualized by immunoblotting, showed distinct differences (Fig. 6F). The preparations contained equal amounts of the mature 8-kDa M protein, arguing that the proteolytic cleavage of the prM precursor was not impaired in the presence of spautin-1. However, an additional band corresponding to the 16-kDa pr peptide was observed from the viral particles assembled in the presence of spautin-1. Thus, the pr peptide, which normally remains associated with the virion within the cell to prevent early fusion events and is released into the extracellular milieu (Fig. 7), was not released in the presence of spautin-1. Presumably, it is the retention of the pr peptide, or the altered virion conformation that prevents its release, that renders the viral particles noninfectious. These data argue that virion maturation is deranged by spautin-1 treatment and is consistent with the increase in the specific infectivity observed in mouse tissue upon the stimulation of autophagy.

DISCUSSION

The present report describes an unprecedented role for autophagy in the infectious cycle of dengue virus: the assembly of infectious particles. Inhibiting autophagy at the stage of beclin-Vps34-Atg14 complex accumulation caused a modest decrease in viral RNA accumulation and a much larger reduction in the production of infectious virions. The smaller amounts of RNA in our experiments are consistent with previous reports (26) but are not sufficient to explain the large decrease in the viral titer that we observed

in the presence of spautin-1. We propose a direct effect of constituents of the autophagy pathway on dengue virus assembly for several reasons. First, the inhibition of infectious dengue virus particle formation by spautin-1 is not reversible by nutritional supplementation. Second, dengue virus RNA-containing particles are still secreted in the presence of spautin-1. Finally, the stimulation of autophagy had the opposite effect from its inhibition: dengue viral particle specific infectivity was greatly increased.

The dependence of dengue virus on cellular autophagy could be direct, such as a requirement for viral RNA packaging on lipidated LC3-II, or indirect, such as the autophagic degradation of some constituent that would otherwise be antiviral or the autophagic provision of some constituent required by the virus. Work by Heaton and Randall established a relationship between autophagy-mediated lipid droplet degradation and dengue virus RNA replication. The role of autophagy was hypothesized to be to provide free fatty acids as an energy source for RNA replication when the pathway was inhibited by 3-MA-reduced RNA levels and titers were rescued by external addition of oleic acid to the cells. However, this is not the case for the defect in virion production observed here, which is not reversed by the provision of oleic acid. Blocking the autophagy pathway with compounds like 3-MA, which inhibits many cellular PI3Ks, renders interpretation of these treatments difficult. Spautin-1 is a potent and selective inhibitor of cellular ubiquitinases USP10 and USP13. The specific destabilization of the beclin-Vps34-Atg14 complex is predicted to inhibit the autophagy pathway at a point upstream of ATG5 or ATG7 knockdowns or knockouts (Fig. 1C) and may therefore affect even autophagy processes that are Atg5 independent (41).

Here, data are presented showing that components or sequelae of cellular autophagy play a critical role in dengue virus assembly. Although without precedent for flaviviruses, recent work by Li et al. has shown that hepatitis B virus, a DNA virus, requires the autophagy pathway for correct viral envelopment, with little or no effect on genome replication or protein translation upon autophagy inhibition (42). For dengue virus, we have shown that the inhibition of autophagy leads to the formation of deranged particles whose prM protein is successfully cleaved but not released to allow the virion to mature. The original defect that prevents this release could be at the level of the formation of the lipid droplets known to be critical for the interactions between dengue virus RNA and core protein, budding of these core-RNA complexes into the endoplasmic reticulum (ER), or any other step at which the structure of the virion is altered so that release of the pr peptide does not occur (Fig. 7). That a similar defect occurs during murine infection is supported by the increase in specific infectivity of virus particles prepared from mice infected in the presence of stimulators of autophagy.

Inhibition of autophagy is currently being considered as a possible therapeutic strategy for diseases, including acute neurological injuries and cancers (19), and could be an attractive target for antivirals, as well. The selection of spautin-1-resistant viruses has proven difficult thus far. One of the advantages of targeting a cellular pathway for antiviral treatments is that it can make the appearance of drug-resistant viruses less likely. Although a functional pathway is likely to be important long term to prevent neurodegeneration (12), its short-term inhibition for acute infections by dengue virus and other autophagy-dependent microbes is promising.

ACKNOWLEDGMENTS

We thank Peter Sarnow and David Constant for comments on the manuscript and Sujana Shrestha and Eva Harris for valuable advice and reagents.

This work was supported by a MEC/Fulbright fellowship to R.M. and NIH Director Pioneer Awards to J.Y. and K.K. and by support from the NIH-supported Pacific Southwest Regional Center for Excellence in Bio-defense and Emerging Pathogens.

REFERENCES

- Schlegel A, Giddings TH, Ladinsky MS, Kirkegaard K. 1996. Cellular origin and ultrastructure of membranes induced during poliovirus infection. *J. Virol.* 70:6576–6588.
- den Boon JA, Diaz A, Ahlquist P. 2010. Cytoplasmic viral replication complexes. *Cell Host Microbe* 8:77–85.
- Welsch S, Miller S, Romero-Brey I, Merz A, Bleck CKE, Walther P, Fuller SD, Antony C, Krijnse-Locker J, Bartenschlager R. 2009. Composition and three-dimensional architecture of the dengue virus replication and assembly sites. *Cell Host Microbe* 5:365–375.
- Martins I, Gomes-Neto F, Faustino A, Carvalho F, Carneiro F, Bozza P, Mohana-Borges R, Castanho M, Almeida F, Santos N, Da Poian A. 2012. The disordered N-terminal region of dengue virus capsid protein contains a lipid droplet-binding motif. *Biochem. J.* 444:405–415.
- Samsa MM, Mondotte JA, Iglesias NG, Assunção-Miranda I, Barbosa-Lima G, Da Poian AT, Bozza PT, Gamarnik AV. 2009. Dengue virus capsid protein usurps lipid droplets for viral particle formation. *PLoS Pathog.* 5:e1000632. doi:10.1371/journal.ppat.1000632.
- Boulant S, Targett-Adams P, McLauchlan J. 2007. Disrupting the association of hepatitis C virus core protein with lipid droplets correlates with a loss in production of infectious virus. *J. Gen. Virol.* 88:2204–2213.
- Masaki T, Suzuki R, Murakami K, Aizaki H, Ishii K, Murayama A, Date T, Matsuura Y, Miyamura T, Wakita T, Suzuki T. 2008. Interaction of hepatitis C virus nonstructural protein 5A with core protein is critical for the production of infectious virus particles. *J. Virol.* 82:7964–7976.
- Miyazawa Y, Atsuzawa K, Usuda N, Watashi K, Hishiki T, Zayas M, Bartenschlager R, Wakita T, Hijikata M, Shimotohno K. 2007. The lipid droplet is an important organelle for hepatitis C virus production. *Nat. Cell Biol.* 9:1089–1097.
- Shavinskaya A, Boulant S, Penin F, McLauchlan J, Bartenschlager R. 2007. The lipid droplet binding domain of hepatitis C virus core protein is a major determinant for efficient virus assembly. *J. Biol. Chem.* 282:37158–37169.
- Shapiro J, Sciaky N, Lee J, Bosshart H, Angeletti RH, Bonifacio JS. 1997. Localization of endogenous furin in cultured cell lines. *J. Histochem. Cytochem.* 45:3–12.
- Yu I-M, Zhang W, Holdaway HA, Li L, Kostyuchenko VA, Chipman PR, Kuhn RJ, Rossman MG, Chen J. 2008. Structure of the immature dengue virus at low pH primes proteolytic maturation. *Science* 319:1834–1837.
- Mizushima N, Komatsu M. 2011. Autophagy: renovation of cells and tissues. *Cell* 147:728–741.
- Dunn WA. 1990. Studies on the mechanisms of autophagy: maturation of the autophagic vacuole. *J. Cell Biol.* 110:1935–1945.
- Noda T, Suzuki K, Ohsumi Y. 2002. Yeast autophagosomes: de novo formation of a membrane structure. *Trends Cell Biol.* 12:231–235.
- Ichimura Y, Kirisako T, Takao T, Satomi Y, Shimonishi Y, Ishihara N, Mizushima N, Tanida I, Kominami E, Ohsumi M, Noda T, Ohsumi Y. 2000. A ubiquitin-like system mediates protein lipidation. *Nature* 408:488–492.
- Sou Y-S, Tanida I, Komatsu M, Ueno T, Kominami E. 2006. Phosphatidylserine in addition to phosphatidylethanolamine is an in vitro target of the mammalian Atg8 modifiers, LC3, GABARAP, and GATE-16. *J. Biol. Chem.* 281:3017–3024.
- Tanida I, Tanida-Miyake E, Komatsu M, Ueno T, Kominami E. 2002. Human Apg3p/Aut1p homologue is an authentic E2 enzyme for multiple substrates, GATE-16, GABARAP, and MAP-LC3, and facilitates the conjugation of hApg12p to hApg5p. *J. Biol. Chem.* 277:13739–13744.
- Kabea Y, Mizushima N, Yamamoto A, Oshitani-Okamoto S, Ohsumi Y, Yoshimori T. 2004. LC3, GABARAP and GATE16 localize to autophagosomal membrane depending on form-II formation. *J. Cell Sci.* 117:2805–2812.
- Mizushima N, Levine B, Cuervo AM, Klionsky DJ. 2008. Autophagy fights disease through cellular self-digestion. *Nature* 451:1069–1075.
- Singh R, Cuervo AM. 2011. Autophagy in the cellular energetic balance. *Cell Metab.* 13:495–504.
- Jackson WT, Giddings TH, Taylor MP, Mulinyawe S, Rabinovitch M, Kopito RR, Kirkegaard K. 2005. Subversion of cellular autophagosomal machinery by RNA viruses. *PLoS Biol.* 3:e156. doi:10.1371/journal.pbio.0030156.
- Suh DA, Giddings TH, Kirkegaard K. 2000. Remodeling the endoplasmic reticulum by poliovirus infection and by individual viral proteins: an autophagy-like origin for virus-induced vesicles. *J. Virol.* 74:8953–8965.
- Taylor MP, Kirkegaard K. 2008. Potential subversion of autophagosomal pathway by picornaviruses. *Autophagy* 4:286–289.
- Dales S, Eggers HJ, Tamm I, Palade GE. 1965. Electron microscopic study of the formation of poliovirus. *Virology* 26:379–389.
- Dreux M, Gastaminza P, Wieland SF, Chisari FV. 2009. The autophagy machinery is required to initiate hepatitis C virus replication. *Proc. Natl. Acad. Sci. U. S. A.* 106:14046–14051.
- Heaton NS, Randall G. 2010. Dengue virus-induced autophagy regulates lipid metabolism. *Cell Host Microbe* 8:422–432.
- Lee Y-R, Lei H-Y, Liu M-T, Wang J-R, Chen S-H, Jiang-Shieh Y-F, Lin Y-S, Yeh T-M, Liu C-C, Liu H-S. 2008. Autophagic machinery activated by dengue virus enhances virus replication. *Virology* 374:240–248.
- Panyasrivani M, Khakpoor A, Wikan N, Smith DR. 2009. Co-localization of constituents of the dengue virus translation and replication machinery with amphisomes. *J. Gen. Virol.* 90:448–456.
- Tanida I, Fukasawa M, Ueno T, Kominami E, Wakita T, Hanada K. 2009. Knockdown of autophagy-related gene decreases the production of infectious hepatitis C virus particles. *Autophagy* 5:937–945.
- Zhang L, Yu J, Pan H, Hu P, Hao Y, Cai W, Zhu H, Yu AD, Xie X, Ma D, Yuan J. 2007. Small molecule regulators of autophagy identified by an image-based high-throughput screen. *Proc. Natl. Acad. Sci. U. S. A.* 104:19023–19028.
- Liu J, Xia H, Kim M, Xu L, Li Y, Zhang L, Cai Y, Norberg HV, Zhang T, Furuya T, Jin M, Zhu Z, Wang H, Yu J, Li Y, Hao Y, Choi A, Ke H, Ma D, Yuan J. 2011. Beclin1 controls the levels of p53 by regulating the deubiquitination activity of USP10 and USP13. *Cell* 147:223–234.
- Balsitis SJ, Williams KL, Lachica R, Flores D, Kyle JL, Mehlhop E, Johnson S, Diamond MS, Beatty PR, Harris E. 2010. Lethal antibody enhancement of dengue disease in mice is prevented by Fc modification. *PLoS Pathog.* 6:e1000790. doi:10.1371/journal.ppat.1000790.
- Tan GK, Ng JKW, Trasti SL, Schul W, Yip G, Alonso S. 2010. A non mouse-adapted dengue virus strain as a new model of severe dengue infection in AG129 mice. *PLoS Negl Trop. Dis.* 4:e672. doi:10.1371/journal.pntd.0000672.
- Zellweger RM, Prestwood TR, Shrestha S. 2010. Enhanced infection of liver sinusoidal endothelial cells in a mouse model of antibody-induced severe dengue disease. *Cell Host Microbe* 7:128–139.
- Horner SM, Park HS, Gale M. 2012. Control of innate immune signaling and membrane targeting by the Hepatitis C virus NS3/4A protease are governed by the NS3 helix $\alpha 0$. *J. Virol.* 86:3112–3120.
- Racaniello VR, Baltimore D. 1981. Cloned poliovirus complementary DNA is infectious in mammalian cells. *Science* 214:916–919.
- Taylor MP, Kirkegaard K. 2007. Modification of cellular autophagy protein LC3 by poliovirus. *J. Virol.* 81:12543–12553.
- Konduru K, Kaplan GG. 2006. Stable growth of wild-type hepatitis A virus in cell culture. *J. Virol.* 80:1352–1360.
- Sir D, Kuo C-F, Tian Y, Liu HM, Huang EJ, Jung JU, Machida K, Ou J-HJ. 2012. Replication of hepatitis C virus RNA on autophagosomal membranes. *J. Biol. Chem.* 287:18036–18043.
- Prestwood TR, Prigozhin DM, Sharar KL, Zellweger RM, Shrestha S. 2008. A mouse-passaged dengue virus strain with reduced affinity for heparan sulfate causes severe disease in mice by establishing increased systemic viral loads. *J. Virol.* 82:8411–8421.
- Nishida Y, Arakawa S, Fujitani K, Yamaguchi H, Mizuta T, Kanaseki T, Komatsu M, Otsu K, Tsujimoto Y, Shimizu S. 2009. Discovery of Atg5/Atg7-independent alternative macroautophagy. *Nature* 461:654–658.
- Li J, Liu Y, Wang Z, Liu K, Wang Y, Liu J, Ding H, Yuan Z. 2011. Subversion of cellular autophagy machinery by hepatitis B virus for viral envelopment. *J. Virol.* 85:6319–6333.